

## Synergy of Turbulent Momentum Drive and Magnetic Braking

R. Varnnes<sup>1</sup>, X. Garbet<sup>1</sup>, L. Vermare<sup>2</sup>, Y. Sarazin<sup>1</sup>, G. Dif-Pradalier<sup>1</sup>, V. Grandgirard,<sup>1</sup>  
 P. Ghendrih,<sup>1</sup> P. Donnel<sup>1</sup>, M. Peret,<sup>1</sup> K. Obrejan<sup>1</sup>, and E. Bourne<sup>1</sup>  
<sup>1</sup>CEA, IRFM, F-13108 Saint-Paul-Lez-Durance, France  
<sup>2</sup>LPP, CNRS, Ecole polytechnique, 91128 Palaiseau, France

 (Received 1 December 2021; revised 17 February 2022; accepted 10 June 2022; published 23 June 2022)

In absence of external torque, plasma rotation in tokamaks results from a balance between collisional magnetic braking and turbulent drive. The outcome of this competition and cooperation is essential to determine the plasma flow. A reduced model, supported by gyrokinetic simulations, is first used to explain and quantify the competition only. The ripple amplitude above which magnetic drag overcomes turbulent viscosity is obtained. The synergetic impact of ripple on the turbulent toroidal Reynolds stress is explored. Simulations show that the main effect comes from an enhancement of the radial electric field shear by the ripple, which in turn impacts the residual stress.

DOI: [10.1103/PhysRevLett.128.255002](https://doi.org/10.1103/PhysRevLett.128.255002)

Mean flows and especially toroidal rotation play a key role in confinement properties of tokamak plasmas. Indeed, numerous experiments have highlighted the link between plasma rotation and improved plasma performance [1–5]. On most medium-size tokamaks, rotation is controllable using the external torque exerted by tangential neutral beam injection. However, in reactor-size tokamaks, including the International Thermonuclear Experimental Reactor (ITER), external torque is expected to be small [6], so that the plasma rotation will likely be driven by intrinsic plasma mechanisms. Intrinsic generation of rotation results from symmetry breaking [7]. Therefore, toroidal asymmetry of the magnetic field plays a leading role in rotation drive, as realistic magnetic configurations always include nonaxisymmetric perturbations. They result from error fields due to coil misalignment, magnetohydrodynamic instabilities, externally applied perturbations, or magnetic field modulations due to the finite number of toroidal coils, called “ripple.” This Letter focuses on the latter. Toroidal magnetic ripple constrains the toroidal torque through magnetic braking, i.e., the force resulting from the magnetic field inhomogeneity on particle magnetic moments. This force substantially changes the plasma rotation even for small amplitude perturbations [8]. The resulting torque, called neoclassical toroidal viscosity, and its impact on toroidal rotation have been experimentally observed [9–13] and widely studied theoretically [14–26] as well as numerically [27–31]. Turbulence can also be responsible for the intrinsic rotation of the plasma. However a symmetry breaking mechanism is also required, which can be either a background  $E \times B$  shear [32], an up-down asymmetry [33], or a shear of turbulent intensity [34]. It has also been extensively studied [7,32–45]. Yet, the possible competing and/or synergetic effects of extrinsic (ripple) versus self-generated (turbulence) asymmetries on rotation has drawn

little [46,47] attention so far. Consequences are of prime importance, since any modification of mean flows impacts the radial electric field and, therefore, also the transition toward improved confinement regimes [48]. In this Letter, the ripple amplitude threshold  $\delta_c$  below which turbulence governs plasma flows is estimated theoretically, first without any crosstalk between ripple and turbulence. It is in agreement with nonlinear gyrokinetic simulations using the GYSELA code [49] and given with a simple expression. Second, the interplay between turbulence and ripple regarding the toroidal velocity is studied thanks to comprehensive gyrokinetic simulations for the first time. The modification of the spectral intensity by ripple through mode coupling is found negligible. However, ripple is found to modify the toroidal Reynolds stress through the radial electric field shear.

Based on the complete toroidal angular momentum conservation [43,50], one can write a simplified expression of the toroidal momentum evolution, keeping the dominant terms. Expressed within the large aspect ratio limit, the ripple and turbulent contributions to the toroidal velocity  $V_T$  evolution read as follows:

$$\partial_t V_T = \mathcal{M} - r^{-1}(r\Pi)', \quad (1)$$

where a prime stands for the derivative along the radial coordinate  $r$ ,  $\mathcal{M}$  is the magnetic braking, and  $\Pi$  is the turbulent radial flux of toroidal momentum, called toroidal Reynolds stress. Each contribution deserves some attention. The magnetic braking is derived within neoclassical theory, i.e., a kinetic derivation describing the resonant enhancement of collisional transport processes. A well-established result of this theory in axisymmetric configurations is the degeneracy between the toroidal velocity  $V_T$  and the radial electric field  $E_r$ . Ripple breaks axisymmetry,

leading to nonambipolar diffusion of particles and heat [14]. The resulting radial electric field constrains the toroidal torque through magnetic braking  $\mathcal{M}$ , removing the degeneracy. The magnetic braking is defined as the following fluid moment of the ion distribution function  $F$ :

$$\mathcal{M} = \frac{-1}{nm} \left\langle \int d^3v R \nabla \varphi \cdot \nabla (\mu \tilde{B}) F \right\rangle, \quad (2)$$

where  $\langle \cdot \rangle$  denotes a flux surface average,  $\varphi$  is the toroidal angle,  $\mu$  is the magnetic moment,  $m$  is the particle mass,  $n$  is the density, and  $R$  is the tokamak major radius. The toroidal perturbation of the magnetic field amplitude due to ripple reads  $\tilde{B} = B(r, \theta) \delta(r, \theta) \cos(N_c \varphi)$ , where  $\theta$  is the poloidal angle,  $B$  is the axisymmetric magnetic field amplitude,  $\delta$  is the ripple amplitude, and  $N_c$  is the number of toroidal coils.  $\mathcal{M}$  is thus the force due to toroidal asymmetry of the magnetic field. It takes the form of a friction [14],

$$\mathcal{M} = -\nu_\varphi (V_T - V_{\text{neo}}), \quad (3)$$

where  $V_{\text{neo}}$  is the target velocity fixed by collisional processes and  $\nu_\varphi$  is the magnetic drag coefficient. The former, roughly independent of  $\delta$ , is in the counterdirection as the nonambipolar particle flux results in a negative  $E_r$  [22,24]. Both  $V_{\text{neo}}$  and  $\nu_\varphi$  are predicted by neoclassical theory. Dedicated simulations including ripple perturbation have found that GYSELA results are consistent with these theoretical predictions. Ripple perturbation implementation in GYSELA is detailed in the Supplemental Material [51]. In the absence of turbulence, the  $V_T$  dynamic is then governed by the magnetic drag coefficient  $\nu_\varphi$ , which depends on the ripple amplitude  $\delta$ . The other drive mechanism is turbulence through the toroidal Reynolds stress  $\Pi$ . Keeping only turbulent contributions, the toroidal component of the stress tensor takes the form [34,36,37]

$$\Pi = -\chi V_T' + \mathcal{V} V_T + \Pi_{\text{res}}, \quad (4)$$

where  $\chi$  is a turbulent viscosity coefficient,  $\mathcal{V}$  is a pinch coefficient, and  $\Pi_{\text{res}}$  is the residual stress. The latter describes the momentum exchange between waves and particles, which acts as the only source of intrinsic plasma rotation in the axisymmetric case. Combining these mechanisms, the equilibrium toroidal velocity  $V_{T\text{eq}}$  reads

$$V_{T\text{eq}} = \frac{\nu_\varphi V_{\text{neo}} - r^{-1} (r \Pi_{\text{res}})'}{\nu_\varphi + \chi \lambda_v + \mathcal{V} \kappa_v}, \quad (5)$$

with  $\lambda_v = -(r \chi V_{T\text{eq}}') / (r \chi V_{T\text{eq}})$  and  $\kappa_v = (r \mathcal{V} V_{T\text{eq}})' / (r \mathcal{V} V_{T\text{eq}})$ . As discussed below, this equation allows one to estimate the ripple amplitude for which magnetic braking overcomes turbulence. Note that any interplay between ripple and turbulence is not considered here, but will be discussed later. Since  $\nu_\varphi$  is an increasing monotonic

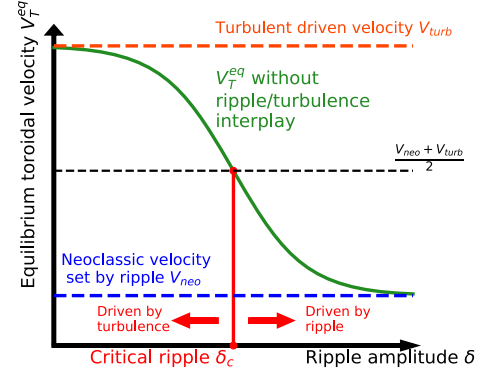


FIG. 1. Sketch of the modeled ripple-turbulence competition on the equilibrium toroidal velocity estimated with local momentum conservation in the case of cocurrent  $V_{\text{turb}}$ . The synergistic effects are not accounted for here, but are detailed further below.

function of the ripple amplitude  $\delta$ , then at low ripple  $\delta \rightarrow 0$ , neoclassical terms vanish so  $V_{T\text{eq}} \rightarrow V_{\text{turb}} = -[r^{-1} (r \Pi_{\text{res}})' / (\chi \lambda_v + \mathcal{V} \kappa_v)]$ . At high ripple  $\delta \rightarrow \infty$ , turbulent terms become negligible so  $V_{T\text{eq}} \rightarrow V_{\text{neo}}$ . Computing the radial profile of  $V_{T\text{eq}}$  as a function of the ripple amplitude requires solving a transport equation. However a “critical ripple” amplitude  $\delta_c$  can be devised such that magnetic braking is dominant when  $\delta > \delta_c$ . As shown Fig. 1, this critical value can be roughly defined as  $V_{T\text{eq}}(\delta_c) = (V_{\text{neo}} + V_{\text{turb}})/2$  leading to  $\nu_\varphi(\delta_c) = |\lambda_v| \chi_{\text{eff}}$  with the effective viscosity defined as  $\chi_{\text{eff}} = \chi + (\kappa_v / \lambda_v) \mathcal{V}$ . As already mentioned, predictions on  $\nu_\varphi$  and its dependence on  $\delta$  are known. Conversely, there are so far no reliable analytical predictions about  $\chi$  and  $\mathcal{V}$ . Determining these coefficients is actually an active topic of both experimental and theoretical research. Here they are determined with four gyrokinetic simulations of ion temperature gradient driven turbulence, performed with adiabatic electrons, of a typical Tore Supra discharge [52] without ripple (i.e.,  $\delta = 0$ ). Details on simulation parameters can be found in the Supplemental Material [51]. Taking advantage of the  $\Pi$  structure Eq. (4), one can determine  $\chi$  and  $\mathcal{V}$  for each radius by initializing the simulations with different toroidal velocity. A least-squares method using the resulting  $V_T$ ,  $V_T'$ , and  $\Pi$  profiles after saturation of turbulence, displayed in Fig. 2, gives access to these coefficients. As indicated by the clear correlation between Reynolds stress and toroidal velocity shear, the viscosity term is dominant. The resulting turbulent viscous contribution to  $V_{T\text{eq}}$  is displayed in Fig. 3 (orange lines). In addition, at  $r/a \approx 0.5$  with  $a$  the minor radius, where  $V_T'$  vanishes and  $V_T$  is extremal,  $\Pi$  reaches the same value for each simulation, whereas the pinch contribution is linear with  $V_T$ . Therefore, the pinch term in these simulated cases is negligible, as already observed in gyrokinetic simulations with adiabatic electrons [7], so that  $\Pi$  is dominated by the residual stress at vanishing  $V_T'$ . In experiments, the pinch contribution can, however, be

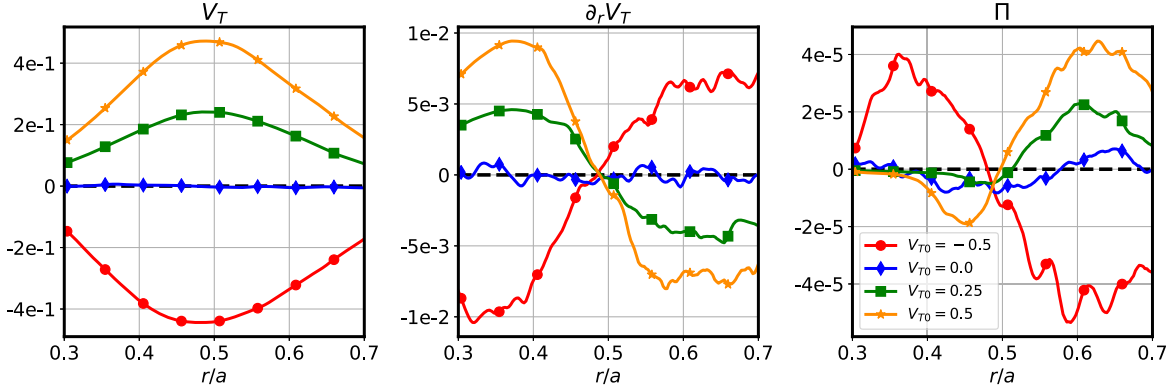


FIG. 2. Radial profiles of the toroidal velocity  $V_T$ , its shear  $V_T'$ , and the stress tensor  $\Pi$  taken at turbulent saturation for simulations without ripple and with different initial toroidal velocity profiles  $V_T(t=0) = V_{T0} \exp[-32(r/a - 0.5)^2]$  with  $a$  the minor radius. Velocities are normalized to the ion thermal velocity and lengths to ion Larmor radius  $\rho_i$ .

significant and actually plays an important role in determining the radial profile of  $V_T$ .

To check the relevance of the prediction regarding  $\delta_c$ , two additional simulations with finite ripple, and consequently, finite magnetic drag, such that  $\nu_\phi \ll \chi|\lambda_v|$  and  $\nu_\phi \gg \chi|\lambda_v|$  were run, cf. Fig. 3 (green and blue lines). Since the physics of the boundary acts as a complex momentum sink, controlled by orbit losses, momentum flux carried by waves [35] and scrape-off layer interactions, a model ripple amplitude is chosen with a radially Gaussian envelope centered at midradius:  $\delta(r) = \delta_0 \exp[-32(r/a - 0.5)^2]$ . This ensures the disentanglement between boundary conditions and intrinsic physics in a controlled way. In these simulations, the midradius ripple amplitudes are  $\delta_0 = 0.1\%$  and  $\delta_0 = 1\%$ . The time evolution of the toroidal velocity  $V_T$  (respectively, of the radial electric field  $E_r$ ) for each case near midradius is shown in Fig. 4(a) [respectively, Fig. 4(b)]. The  $\delta_0 = 0.1\%$  case exhibits no significant difference with the axisymmetric case  $\delta_0 = 0\%$ , neither regarding  $V_T$  nor  $E_r$ . Conversely, the toroidal velocity in

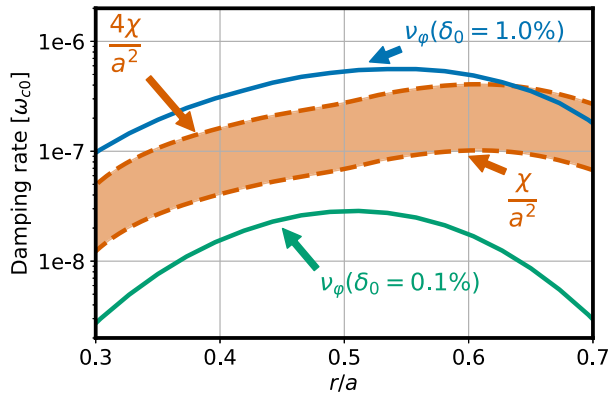


FIG. 3. Radial profile of magnetic drag  $\nu_\phi$  for different ripple amplitudes and the turbulent viscous contribution  $\chi\lambda_v$ . Orange zone represents  $\chi|\lambda_v|$  for  $a/2 \leq |\lambda_v|^{-1/2} \leq a$ . Time is normalized to the cyclotron period  $\omega_{c0}^{-1}$ .

the  $\delta_0 = 1\%$  case, deeply in the countercurrent direction, is driven by magnetic braking. Also,  $E_r$  increases roughly by a factor 1.5. The critical ripple amplitude then stands out as a practical landmark to determine the main driving flow mechanism. All the elements of the relation  $\nu_\phi(\delta_c) = |\lambda_v|\chi_{\text{eff}}$  may not be known, in particular, because the viscosity and pinch profiles are difficult to obtain experimentally. One can then use the following rule of thumb to evaluate the order of magnitude of  $\delta_c$ . First, one can fairly approximate the magnetic drag to its asymptotic value in the so-called “ripple-plateau” regime of collisionality. In most tokamaks, including ITER, this regime is the most relevant and states that  $\nu_\phi \sim (N_c V_{\text{th}}/R)\delta^2$ , where  $V_{\text{th}}$  is the ion thermal velocity. There is more uncertainty regarding a proxy for the effective viscosity. One can nevertheless consider the gyro-Bohm scaling  $\chi_{\text{eff}} \sim (\rho_i^2 V_{\text{th}}/L_T)$ , where  $L_T$  is the temperature gradient length and  $\rho_i$  is the ion

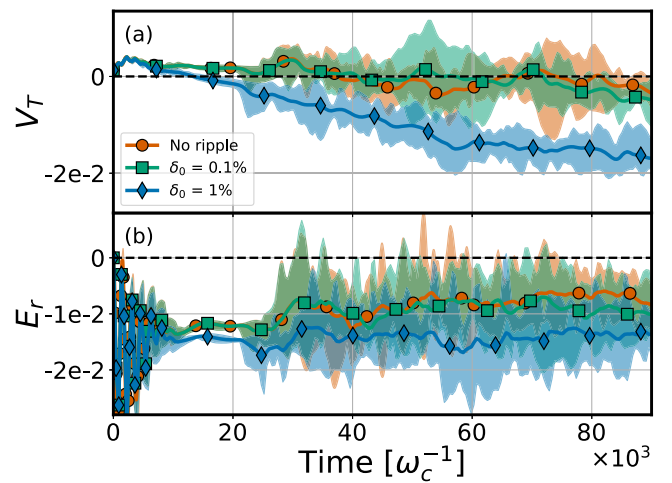


FIG. 4. Time trace of the (a) toroidal velocity  $V_T$  and (b) the radial electric field  $E_r$  for different ripple amplitudes in  $0.45 < r/a < 0.55$ , shaded areas, and radially averaged in this same interval, solid lines.

Larmor radius. The validity of these approximations was verified with GYSELA simulations and is detailed in the Supplemental Material [51]. Magnetic braking follows the standard neoclassical theory and the gyro-Bohm scaling fits the turbulent viscosity in magnitude. Under these hypotheses, the critical ripple amplitude can be estimated as  $\delta_c \sim \rho_* \varepsilon [(1/N_c)(R/L_T)R^2 |\lambda_v|]^{1/2}$ , where  $\varepsilon$  is the inverse aspect ratio and  $\rho_* = \rho_i/a$ . A naive application on a Tore Supra Ohmic discharge at  $r/a = 0.8$  with  $\rho_*^{-1} = 700$ ,  $R/L_T = 12$ ,  $N_c = 18$ , and  $|\lambda_v|^{-1/2} \sim 20$  cm [53] gives  $\delta_c \approx 0.4\%$ , which is way lower than the actual ripple amplitude in Tore Supra at this location. Consistently, the equilibrium rotation and radial electric field are found to be ruled by ripple [54]. So far, magnetic braking and turbulent stress were computed separately, ignoring any crosstalk. Each mechanism of backreaction between turbulence and magnetic braking is studied using three simulations performed with different ripple amplitudes. On the one hand, based on Eq. (2), the effect of turbulence on magnetic braking  $\mathcal{M}$  is observed to be negligible, as ripple wave numbers are nonresonant, and hence hardly generated via mode coupling. On the other hand, the magnetic braking is found to impact the turbulent momentum transport  $-r^{-1}(r\Pi)'$ . It is known that the residual stress is predicted to depend on the turbulent intensity shear and the  $E \times B$  drift shear [34,36], while turbulent viscosity depends only on the former. The residual stress can be expressed as

$$\Pi_{\text{res}} = \sum_k k_{\parallel} k_{\theta} \left| \frac{e\phi_k}{T} \right|^2 \tau_k, \quad (6)$$

where  $\phi_k$  are the Fourier components of the electric potential,  $T$  is the thermal energy,  $k_{\parallel}$  and  $k_{\theta}$  are the parallel and poloidal wave number, and  $\tau_k$  is a form factor [55]. The modification of the spectral intensity  $|\phi_k|^2$  by ripple through mode coupling in simulations is found negligible for large-scale modes. This implies that the turbulent viscosity is not affected by ripple. However the  $E \times B$  shear modifies the parallel wave number by introducing radial asymmetry [38]. Ripple increases the radial electric field amplitude through neoclassical effects, so the  $E_r$  shear depends on the radial shape of the ripple amplitude. The model  $\Pi_{\text{res}}$  from Eq. (6) comes from a mean field theory that holds when  $E_r$  is averaged over multiple turbulent structure lengths and correlation times, defining the coarse-grained average labeled  $\langle \cdot \rangle_{\text{CG}}$ . This is done by time averaging over  $10^5$  cyclotron periods, i.e., about 50 correlation times, and performing a sliding radial average with a  $50\rho_i$  window, i.e., about 5–6 correlation lengths. Mean  $E_r$  and associated shear are plotted in Figs. 5(a) and 5(b). The effect of ripple on these profiles is clear: both  $\langle E_r \rangle_{\text{CG}}$  and  $\langle E_r' \rangle_{\text{CG}}$  increase in amplitude with  $\delta$  near the core region. The residual stress profile in Fig. 5(c) is calculated as  $\Pi_{\text{res}} = \Pi + \chi V_T'$  using the previously obtained viscosity. As the initial toroidal velocity in these simulation is zero, the viscous term is subdominant. It then appears that  $\Pi_{\text{res}}$

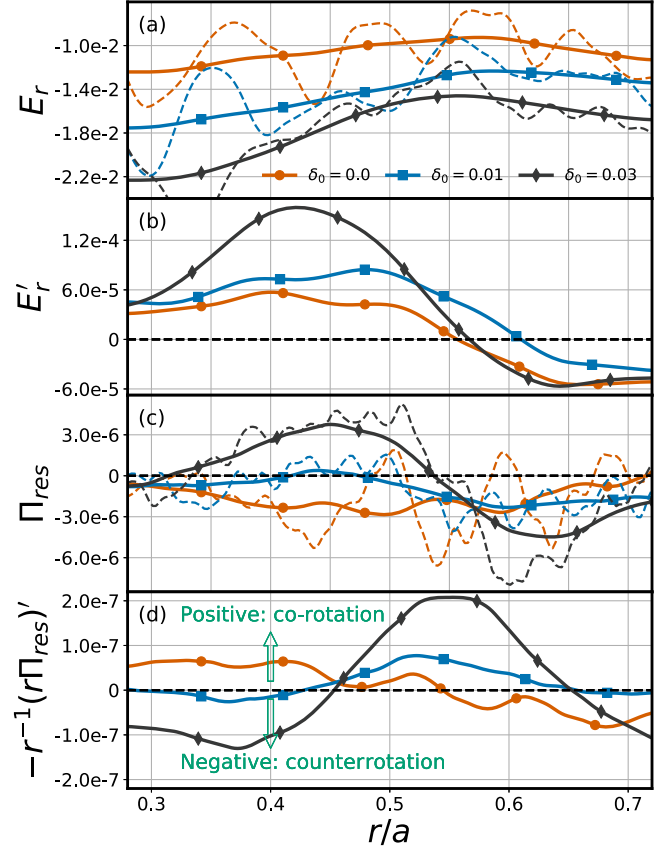


FIG. 5. Solid lines, radial profile of coarse-grained (temporally and spatially) (a) radial electric field and (b) its shear, as well as (c) residual stress and (d) the opposite of its divergence for different ripple amplitudes. Dashed lines, time average only.

grows monotonically with  $\delta$  and changes sign.  $\langle E_r' \rangle_{\text{CG}}$  is correlated with the increase of  $\langle \Pi_{\text{res}} \rangle_{\text{CG}}$  up to an offset, consistent with the numerical study [56]. The offset is likely explained by the impact of turbulent intensity shear and also by the effect of diamagnetism [34]. Finally, Fig. 5(d) shows the averaged  $-r^{-1}(r\Pi)'$  that appears in momentum conservation, Eq. (1). Regarding plasma rotation, positive and negative values of  $\langle E_r'' \rangle_{\text{CG}}$  are found correlated with an increment of the toroidal velocity in the counter- and cocurrent direction respectively due to turbulence. The critical ripple expression, derived without interplay, is still valid as it does not depend on the residual stress.

In summary, the effect of turbulent drive and magnetic braking has been studied on the same footing thanks to comprehensive gyrokinetic simulations. The critical ripple amplitude for which magnetic braking overcomes turbulence has been estimated theoretically and agrees with gyrokinetic simulations. An estimate for this threshold is proposed and its value in Tore Supra agrees with experimental measurements. Ripple also modifies the toroidal velocity by changing the turbulent Reynolds stress through the residual stress. In fact, the toroidal Reynolds stress is observed to vary monotonically with the ripple amplitude.

It is observed in simulations that  $E_r'$  is enhanced in the presence of ripple and that  $E_r'$  controls the residual stress. Robust knowledge of this intrinsic physics provides means to control the rotation. Indeed, recent work [57] demonstrated that restoring the magnetic symmetry is actually possible, giving some leverage on the magnetic braking strength.

The authors want to thank P. Diamond and C. Chen for helpful contributions. This work has been carried out within the framework of the EUROfusion Consortium, funded by the European Union via the Euratom Research and Training Program (Grant Agreement No. 101052200—EUROfusion). Views and opinions expressed are, however, those of the author(s) only and do not necessarily reflect those of the European Union or the European Commission. Neither the European Union nor the European Commission can be held responsible for them. This work was performed using HPC resources from GENCI, CCRT-TGCC, and CINECA. This work was supported by funding from the European Union's Horizon 2020 research and innovation program under Grant Agreement No. 824158 (EoCoE II).

- 
- [1] P. Mantica, D. Strintzi, T. Tala, C. Giroud, T. Johnson, H. Leggate, E. Lerche, T. Loarer, A. G. Peeters, A. Salmi, S. Sharapov, D. VanEester, P. C. de Vries, L. Zabeo, and K. D. Zastrow, *Phys. Rev. Lett.* **102**, 175002 (2009).
- [2] P. C. de Vries, G. Waidmann, A. J. H. Donn e, and F. C. Sch uller, *Plasma Phys. Controlled Fusion* **38**, 467 (1996).
- [3] T. S. Hahm and K. H. Burrell, *Phys. Plasmas* **2**, 1648 (1995).
- [4] Y. Sakamoto *et al.*, *Nucl. Fusion* **41**, 865 (2001).
- [5] M. F. F. Nave, T. Johnson, L. G. Eriksson, K. Crombe, C. Giroud, M. L. Mayoral, J. Ongena, A. Salmi, T. Tala, and M. Tsalias (JET-EFDA Contributors), *Phys. Rev. Lett.* **105**, 105005 (2010).
- [6] M. Rosenbluth and F. Hinton, *Nucl. Fusion* **36**, 55 (1996).
- [7] A. Peeters *et al.*, *Nucl. Fusion* **51**, 094027 (2011).
- [8] H. Urano, N. Oyama, K. Kamiya, Y. Koide, H. Takenaga, T. Takizuka, M. Yoshida, and Y. Kamada (the JT-60 Team), *Nucl. Fusion* **47**, 706 (2007).
- [9] W. Zhu, S. A. Sabbagh, R. E. Bell, J. M. Bialek, M. G. Bell, B. P. LeBlanc, S. M. Kaye, F. M. Levinton, J. E. Menard, K. C. Shaing, A. C. Sontag, and H. Yuh, *Phys. Rev. Lett.* **96**, 225002 (2006).
- [10] J.-K. Park, A. H. Boozer, J. E. Menard, A. M. Garofalo, M. J. Schaffer, R. J. Hawryluk, S. M. Kaye, S. P. Gerhardt, and S. A. Sabbagh, *Phys. Plasmas* **16**, 056115 (2009).
- [11] Y. Sun *et al.*, *Plasma Phys. Controlled Fusion* **52**, 105007 (2010).
- [12] A. J. Cole, J. D. Callen, W. M. Solomon, A. M. Garofalo, C. C. Hegna, M. J. Lancotot, and H. Reimerdes, *Phys. Plasmas* **18**, 055711 (2011).
- [13] C. Fenzi *et al.*, *Nucl. Fusion* **51**, 103038 (2011).
- [14] X. Garbet *et al.*, *Phys. Plasmas* **17**, 072505 (2010).
- [15] L. Kovrizhnykh, *Nucl. Fusion* **24**, 851 (1984).
- [16] V. S. Tsypin, A. B. Mikhailovskii, R. M. O. Galv o, I. C. Nascimento, M. Tendler, C. A. de Azevedo, and A. S. de Assis, *Phys. Plasmas* **5**, 3358 (1998).
- [17] K. C. Shaing, *Phys. Fluids* **26**, 3315 (1983).
- [18] K. C. Shaing, J. A. Rome, and R. H. Fowler, *Phys. Fluids* **27**, 1 (1984).
- [19] K. C. Shaing, S. P. Hirshman, and J. D. Callen, *Phys. Fluids* **29**, 521 (1986).
- [20] K. C. Shaing, *Phys. Rev. Lett.* **76**, 4364 (1996).
- [21] T. E. Stringer, *Phys. Fluids* **14**, 2177 (1971).
- [22] J. Connor and R. Hastie, *Nucl. Fusion* **13**, 221 (1973).
- [23] P. Yushmanov, *Nucl. Fusion* **22**, 315 (1982).
- [24] P. Yushmanov, *Nucl. Fusion* **23**, 1599 (1983).
- [25] P. Yushmanov, J. R. Cary, and S. G. Shasharina, *Nucl. Fusion* **33**, 1293 (1993).
- [26] P. N. Yushmanov, *Reviews of Plasma Physics*, edited by B. B. Kadomtsev (Consultants Bureau, New York, 1991).
- [27] S. Matsuoka, Y. Idomura, and S. Satake, *Phys. Plasmas* **24**, 102522 (2017).
- [28] S. Satake, Y. Idomura, H. Sugama, and T.-H. Watanabe, *Comput. Phys. Commun.* **181**, 1069 (2010).
- [29] S. Satake, J. K. Park, H. Sugama, and R. Kanno, *Phys. Rev. Lett.* **107**, 055001 (2011).
- [30] N. C. Logan, J.-K. Park, K. Kim, Z. Wang, and J. W. Berkery, *Phys. Plasmas* **20**, 122507 (2013).
- [31] K. Kim, J.-K. Park, A. H. Boozer, J. E. Menard, S. P. Gerhardt, N. C. Logan, Z. R. Wang, G. J. Kramer, K. H. Burrell, and A. M. Garofalo, *Nucl. Fusion* **54**, 073014 (2014).
- [32] P. H. Diamond *et al.*, in *Proceedings of the 15th International Conference on Plasmas Physics and Controlled Nuclear Fusion*, Seville (IAEA, Vienna, 1994).
- [33] Y. Camenen, A. G. Peeters, C. Angioni, F. J. Casson, W. A. Hornsby, A. P. Snodin, and D. Strintzi, *Phys. Rev. Lett.* **102**, 125001 (2009).
- [34]  . D. G urcan, P. H. Diamond, and T. S. Hahm, *Phys. Rev. Lett.* **100**, 135001 (2008).
- [35] P. Diamond, C. J. McDevitt,  . D. G urcan, T. S. Hahm, W. X. Wang, E. S. Yoon, I. Holod, Z. Lin, V. Naulin, and R. Singh, *Nucl. Fusion* **49**, 045002 (2009).
- [36] T. S. Hahm, P. H. Diamond, O. D. Gurcan, and G. Rewoldt, *Phys. Plasmas* **14**, 072302 (2007).
- [37] A. G. Peeters, C. Angioni, and D. Strintzi, *Phys. Rev. Lett.* **98**, 265003 (2007).
- [38]  . D. G urcan, P. Diamond, T. S. Hahm, and R. Singh, *Phys. Plasmas* **14**, 042306 (2007).
- [39] W. Solomon *et al.*, *Nucl. Fusion* **49**, 085005 (2009).
- [40] F. J. Casson, A. G. Peeters, Y. Camenen, W. A. Hornsby, A. P. Snodin, D. Strintzi, and G. Szepesi, *Phys. Plasmas* **16**, 092303 (2009).
- [41] M. Barnes, F. I. Parra, J. P. Lee, E. A. Belli, M. F. F. Nave, and A. E. White, *Phys. Rev. Lett.* **111**, 055005 (2013).
- [42] K. Ida and J. Rice, *Nucl. Fusion* **54**, 045001 (2014).
- [43] Y. Idomura, *Phys. Plasmas* **21**, 022517 (2014).
- [44] Y. Idomura, *Phys. Plasmas* **24**, 080701 (2017).
- [45] R. E. Waltz, G. M. Staebler, and W. M. Solomon, *Phys. Plasmas* **18**, 042504 (2011).
- [46] C.-C. Chen, P. H. Diamond, R. Singh, and S. M. Tobias, *Phys. Plasmas* **28**, 042301 (2021).

- [47] R. E. Waltz and F. L. Waelbroeck, *Phys. Plasmas* **19**, 032508 (2012).
- [48] P. W. Terry, *Rev. Mod. Phys.* **72**, 109-165 (2000).
- [49] V. Grandgirard *et al.*, *Comput. Phys. Commun.* **207**, 35-68 (2016).
- [50] J. Abiteboul, X. Garbet, V. Grandgirard, S. J. Allfrey, Ph. Ghendrih, G. Latu, Y. Sarazin, and A. Strugarek, *Phys. Plasmas* **18**, 082503 (2011).
- [51] See Supplemental Material at <http://link.aps.org/supplemental/10.1103/PhysRevLett.128.255002> for further details on the simulation parameters and justification of approximations.
- [52] L. Vermare, P. Hennequin, Ö. D. Gürçan, C. Bourdelle, F. Clairet, X. Garbet, and R. Sabot, *Phys. Plasmas* **18**, 012306 (2011).
- [53] B. Chouli *et al.*, *Plasma Phys. Controlled Fusion* **57**, 125007 (2015).
- [54] E. Trier, L.-G. Eriksson, P. Hennequin, C. Fenzi, C. Bourdelle, G. Falchetto, X. Garbet, T. Aniel, F. Clairet, and R. Sabot, *Nucl. Fusion* **48**, 092001 (2008).
- [55] X. Garbet, Y. Sarazin, P. Ghendrih, S. Benkadda, P. Beyer, C. Figarella, and I. Voitsekhovitch, *Phys. Plasmas* **9**, 3893 (2002).
- [56] W. X. Wang, T. S. Hahm, S. Ethier, G. Rewoldt, W. W. Lee, W. M. Tang, S. M. Kaye, and P. H. Diamond, *Phys. Rev. Lett.* **102**, 035005 (2009).
- [57] J.-K. Park, S. M. Yang, N. C. Logan, Q. Hu, C. Zhu, M. C. Zarnstorff, R. Nazikian, C. Paz-Soldan, Y. M. Jeon, and W. H. Ko, *Phys. Rev. Lett.* **126**, 125001 (2021).